



CrossMark
 click for updates

Cite this: *Soft Matter*, 2015,
 11, 8661

Rate-dependence of 'wet' biological adhesives and the function of the pad secretion in insects†

David Labonte* and Walter Federle

Many insects use soft adhesive footpads for climbing. The surface contact of these organs is mediated by small volumes of a liquid secretion, which forms thin films in the contact zone. Here, we investigate the role of viscous dissipation by this secretion and the 'bulk' pad cuticle by quantifying the rate-dependence of the adhesive force of individual pads. Adhesion increased with retraction speed, but this effect was independent of the amount of pad secretion present in the contact zone, suggesting that the secretion's viscosity did not play a significant role. Instead, the rate-dependence can be explained by relating the strain energy release rate to the speed of crack propagation, using an established empirical power law. The 'wet' pads' behaviour was akin to that of 'dry' elastomers, with an equilibrium energy release rate close to that of dry van-der-Waals contacts. We suggest that the secretion mainly serves as a 'release layer', minimising viscous dissipation and thereby reducing the time- and 'loading-history'-dependence of the adhesive pads. In contrast to many commercial adhesives which derive much of their strength from viscous dissipation, we show that the major modulator of adhesive strength in 'wet' biological adhesive pads is friction, exhibiting a much larger effect than retraction speed. A comparison between 'wet' and 'dry' biological adhesives, using both results from this study and the literature, revealed a striking lack of differences in attachment performance under varying experimental conditions. Together, these results suggest that 'wet' and 'dry' biological adhesives may be more similar than previously thought.

Received 17th June 2015,
 Accepted 10th September 2015

DOI: 10.1039/c5sm01496d

www.rsc.org/softmatter

Introduction

Many arthropods and small vertebrates possess the ability to climb on smooth inverted substrates using adhesive pads located on their legs. In tree frogs, spiders, and insects, the adhesive contact is mediated *via* thin films of a liquid secretion.^{1–13} The presence of a pad secretion is often used to distinguish between these 'wet' adhesives and their 'dry' counterparts in pad-bearing lizards. Despite several previous studies, the secretion's detailed function has remained largely unclear.^{14–16}

One of the frequently discussed functional implications of a 'wet' adhesive is the potential contribution of viscous forces to friction, adhesion, and the contact formation in general.^{4,9,16–28} Indeed, the (dynamic) attachment forces of insects have been shown to decrease with temperature, suggesting that the viscosity of the pad secretion may play a significant role.^{17,21,23} In addition, the adhesive pads themselves have been shown to be viscoelastic,^{29,30–32} but the functional relevance of this property again remains unclear.

Energy dissipation *via* viscous material flow is a major contributor to the strength and toughness of many soft synthetic

adhesives.^{33–35} However, a significant contribution of viscous forces may also have undesirable consequences, in particular for adhesives used during locomotion. For example, detachment in the presence of a liquid requires considerable work, in contrast to 'dry' contacts where this work can be close to the thermodynamic work of adhesion. Viscous forces introduce a time- and load-history dependence of adhesive strength and toughness, which may limit locomotion speed, and can also compromise the structural integrity and thus re-usability of the pads. From this perspective, it may be advantageous to limit viscous energy dissipation, and instead use different mechanisms to modulate adhesive strength during locomotion.

Here, we address the role of viscous dissipation in the 'wet' adhesive pads of Indian stick insects (*Carausius morosus*), and focus on the following questions

- i. How does adhesive force vary with retraction speed?
- ii. How does the amount of fluid present in the contact zone influence the relationship between retraction speed and adhesive force?
- iii. Does the viscoelastic pad material itself contribute to the relationship between retraction speed and adhesive force?

In order to account for viscous dissipation in the deformable pad itself, we model the detachment using fracture mechanics, which we briefly outline in the following section.

Department of Zoology, University of Cambridge, UK. E-mail: dl416@cam.ac.uk

† Electronic supplementary information (ESI) available. See DOI: 10.1039/c5sm01496d



A fracture mechanics approach to insect adhesion

In fracture mechanics, the perimeter of an adhesive contact can be treated as a crack. During detachment, this crack advances, *i.e.* the contact area A between the pad and the surface decreases incrementally, and as a result the amount of elastic and potential mechanical energy stored in the materials changes. The variation of the elastic and mechanical potential energy with A is called strain energy release rate G :

$$\frac{\partial U_A}{\partial A} = \frac{\partial U_E}{\partial A} + \frac{\partial U_{MP}}{\partial A} = G \quad (1)$$

where U_E is the elastic energy of the system, U_{MP} is the mechanical potential energy, and U_A is the energy required to form the adhesive interface. Under true equilibrium conditions $\frac{\partial U_A}{\partial A} = G_0$, where G_0 is the thermodynamic work of adhesion. Breaking adhesive bonds requires the work $G_0 dA$, and the excess $-(G - G_0) dA$ is transformed into kinetic energy if there is no dissipation. $G - G_0$ can thus be interpreted as a crack extension force (per unit crack length), and large values imply that the crack propagates through the interface with high speed. This can result in high strain rates at the crack tip which may trigger a viscoelastic material response, dampening a further increase in the speed of crack propagation. Notably, as long as the expenditure of energy is limited to a region that is small in comparison to the elastically deformed sample, the relationship between load, displacement and contact radius can be accurately described by a single elastic constant for the bulk pad material, and thus eqn (1) is still valid.^{36,37} The contributions of the viscoelastic 'bulk' and the adhesive interface to the crack extension force can be separated using an established empirical law, which relates the crack extension force to the speed of crack propagation v_c .³⁷⁻⁴⁵

$$G - G_0 = G_0 \phi(a_t v_c) = G_0 \left(\frac{v_c}{v^*} \right)^n \quad (2)$$

Here, G_0 is the critical energy release rate as v_c approaches zero, $\phi(a_t v_c)$ is a viscoelastic 'loss function', proportional to G_0 , and a_t is the Williams-Landel-Ferry shift factor for time-temperature superposition. In this work, we use a specific form of the viscoelastic 'loss function', $\phi = (v_c/v^*)^n$, where v^* is a characteristic crack speed at which $G = 2G_0$, and n is an empirical constant.^{37,43-46} Note the simplifying assumption that G_0 is rate-independent. Eqn (2) is valid independent of probe geometry, illustrating the advantage of fracture mechanics.³⁶

Adhesive pads of stick insects are irregularly shaped, with a bean-shaped contact area, and an accurate quantitative expression for G is, to our knowledge, not available. In order to circumvent this problem, we study the variation of the relative energy dissipation, $G/G_0 - 1$, for three common contact geometries. We are making the simplifying assumption that for each geometry, the adhesion force P is described by a single equation containing a velocity-dependent energy release rate G . Thus, for a circular flat punch (assuming an approximately constant elastic modulus), $G/G_0 \approx P(v_c)^2/P_0^2$,⁴⁷ while for an adhesive tape and a spherical indenter, $G/G_0 \approx P(v_c)/P_0$, respectively.^{48,49} Here,

$P(v_c)$ is the peak adhesive force measured at a finite crack speed v_c , and P_0 is the peak adhesive force required to detach the pad under true equilibrium conditions (*i.e.* $v_c = 0$). Thus, if P , v_c , and P_0 are known, the scaling of the relative energy dissipation with crack speed can be assessed without any specific assumptions regarding the stiffness or size of the pads.

Materials and methods

Study animals and set-up

Adult Indian stick insects (*Carausius morosus*, Phasmatidae, Sinéty 1901, body mass: 0.80 ± 0.1 g, mean \pm standard deviation, $n = 21$) were taken from laboratory colonies fed with bramble, ivy and water *ad libitum*. Prior to force measurements, stick insects were slid into glass tubes, and one of the two protruding front legs was attached to a supporting metal wire, so that the ventral side of the arolium was the highest point.⁵⁰

Peak adhesion of individual arolia of live insects was measured using a custom-built fibre-optic 1D-force transducer. A small piece of reflective foil was glued onto one end of a brass plate cut to $100 \times 10 \times 0.2$ mm (length \times width \times thickness), and the opposite end of the plate was clamped onto a metal support with a free-standing length of 30 mm (see Fig. 1A). The metal support was fixed to a 3D motor positioning stage (M-126PD, Physik Instrumente, Karlsruhe, Germany, resolution $0.25 \mu\text{m}$, maximum velocity 15 mm s^{-1}), controlled by a custom-made Labview programme (National Instruments, Austin, TX, USA). The end of a D12 fibre optic sensor (Philtex, INC., Annapolis, USA) was slowly lowered towards the reflective foil, using a micro-manipulator mounted on a custom-built holder (see Fig. 1A). The optical peak of the sensor signal was set to 5 V, using the built-in amplification factor of the sensor's amplifier. The fibre optic sensor was then lowered further until the distance between the tip and the reflective foil was approximately $77 \mu\text{m}$ (equivalent to around 2.2 V), corresponding to the middle of the linear range of the sensor's highly sensitive near-field. An external circuit was used to offset the voltage to 0 V.

The fibre-optic force transducer had a spring constant of $14\text{--}17 \text{ N m}^{-1}$ (depending on the effective lever arm), a resonance frequency of 60 Hz (approximately three times faster than the shortest force peaks measured in this study), and a resolution of $20 \mu\text{N}$, corresponding to around 30% of the smallest adhesive force measured in this study. The output of the fibre optic sensor was recorded at 50 Hz *via* a data acquisition board (PCI-6035E, National Instruments), and at 1000 Hz using a 2020 PicoScope oscilloscope (Pico Technology Ltd, Neots, Cambridgeshire, UK). The 50 Hz signal was used as the input for a force-feedback algorithm implemented in the Labview software, while force data for analysis were extracted from the 1000 Hz signal (see ESI† for representative force-time curves). In the range of velocities used in this study, the z-motor movement was linear (average $R^2 > 0.99$), and the actual speed was within $\pm 3\%$ of the prescribed velocities.

All measurements were performed with glass coverslips ($18 \text{ mm} \times 18 \text{ mm} \times 0.14 \text{ mm}$), which were cleaned before the experiments in an ultrasonic bath (FB 15051, Fisher Scientific,



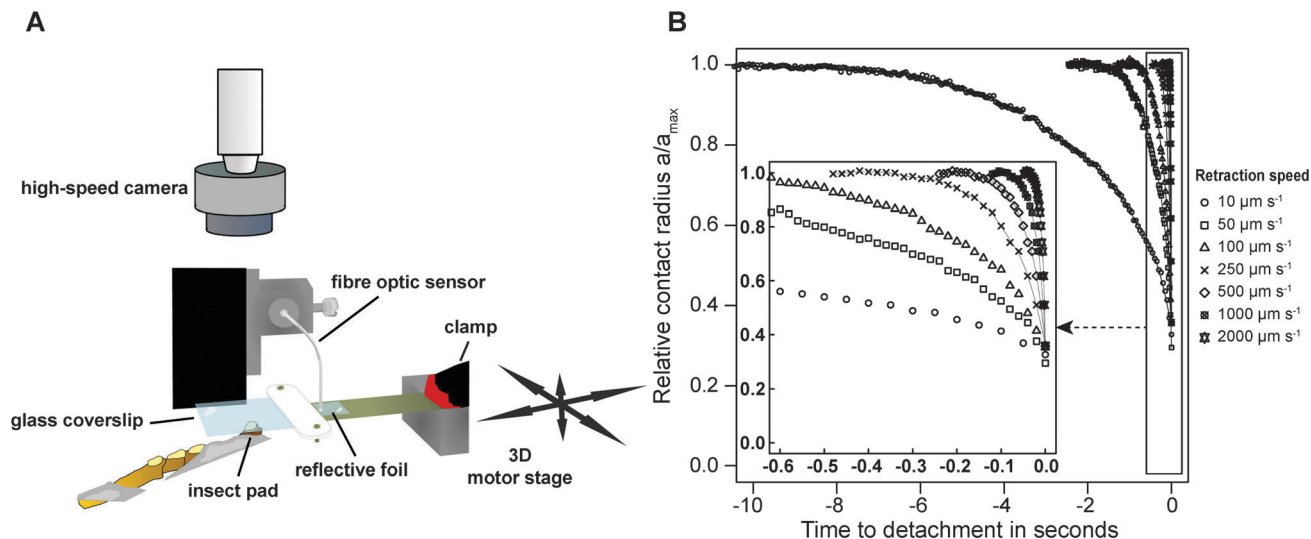


Fig. 1 (A) Schematic of the set-up used to measure the adhesive force of individual pads of live insects for different retraction speeds. (B) Example data of the relative contact radius during detachment with different retraction speeds. The inset shows a zoomed view of the time just before detachment (frame), for better illustration of the faster pull-offs. The lines are the result of a LOESS fit with span 0.3, and their slope is equivalent to the relative speed of crack propagation.

Loughborough, UK) in acetone, and isopropanol (both Fisher Scientific), followed by a rinsing step with de-ionized water and blow-drying with nitrogen. Measurements were performed at ambient conditions (22–25 °C, 40–55% relative humidity) to avoid a systematic influence of temperature or humidity on adhesion.^{23,51}

Experimental protocol

Influence of retraction speed on adhesion. The glass coverslips were attached to the force transducer (see Fig. 1A), and were brought into contact with the pads with a normal preload of 1 mN for a period of 5 s, controlled *via* the force-feedback algorithm incorporated in the Labview programme (arolium adhesion on smooth surfaces is independent of normal preloads between 0.5–4 mN, see ref. 50). The glass coverslip was subsequently retracted with one of seven different motor speeds, ranging from 10–2000 $\mu\text{m s}^{-1}$ (see Table 1, $n = 16$).

Adhesion was measured for all seven retraction speeds per arolium, with a time between detachment and subsequent re-attachment of at least 3 s. The order of the retraction speeds was randomized and each measurement was conducted on a ‘fresh’ spot, in order to avoid a systematic effect of fluid depletion or accumulation on the relationship between peak adhesion and

retraction speed.⁵² During the measurements, the contact area of the pads was filmed using a TTL-triggered Redlake PCI 1000 B/W high-speed camera (Redlake MASD LLC, San Diego, CA, USA), mounted on a stereo-microscope with coaxial illumination (Wild M3C, Leica, Wetzlar, Germany, see ESI† for a representative video). Table 1 shows the frame rate of the recordings for the different retraction speeds.

Interaction between fluid accumulation/depletion and retraction speed. In order to systematically investigate how the amount of pad secretion influences adhesion and its dependence on retraction speed, peak adhesion was also measured in an ‘accumulated’ and a ‘depleted’ fluid condition.⁵² Adhesion measurements were repeated as described above, but with nine consecutive times per pad on either ‘fresh’ spots (depleted), or repeatedly on the same spot (accumulated), each for three different retraction speeds (50, 250, 1000 $\mu\text{m s}^{-1}$), and 10 different insects. Between two measurement series of the same pad (*i.e.* nine consecutive detachments), a time of at least 20 min was allowed, to provide sufficient time for the depleted pads to recover their maximum footprint volume.⁵³

Interaction between shear-sensitivity and retraction speed. The adhesive strength of stick insect pads has been shown to increase with the shear-force acting on the pads during detachment.⁵⁰ A custom-made 2D strain-gauge force transducer was used to measure the combined effect of shear force and retraction speed on arolium adhesion, following the procedure described in detail in ref. 50. Pads of 6 different stick insects were brought in contact with a glass coverslip as described above, after which a shear-force of 1, 2 or 4 mN was applied for 3 s, using the force-feedback algorithm implemented in the Labview control software. The coverslips were then retracted at one of three speeds (250, 500 or 1000 $\mu\text{m s}^{-1}$), and both the peak adhesion and the shear force at this peak adhesion were extracted from the 50 Hz data recorded by the Labview software.

Table 1 Overview of the retraction speeds and corresponding video recording rates

| Retraction speed in $\mu\text{m s}^{-1}$ | Frames per second |
|--|-------------------|
| 10 | 20 |
| 50 | 50 |
| 100 | 50 |
| 250 | 50 |
| 500 | 100 |
| 1000 | 200 |
| 2000 | 500 |



Data analysis

Peak adhesion for all experiments performed with the fibre-optic sensor was extracted from the 1000 Hz force–time data using custom-made Matlab scripts (The Mathworks, Natick, MA, USA). Video recordings were post-processed using Fiji.⁵⁴ The flickering of the light source visible at frame rates > 200 fps was removed by normalising the grey level of all images to the average grey value of the first frame, and the recordings were subsequently converted into binary images, using a ‘fuzzy threshold’ algorithm.⁵⁵ The binary images were de-speckled using 2×2 median filters, and the contact area A , perimeter Γ , width (lateral), height (proximal–distal) and coordinates of a bounding rectangle around the arolia were measured from the videos, using the native particle analysis routines implemented in Imagejv1.48k. All contact area parameters were smoothed with a second order LOESS-algorithm (span = 0.3). In order to compensate for the decrease in resolution with increasing detachment speed, the detachment time was divided into 200 steps, and the LOESS-fit was used to predict the contact area parameters at these steps from the original data (see Fig. 1B).

Speed of crack propagation and mode of detachment. We use concepts from fracture mechanics (see above), and treat the contact perimeter as a crack. During detachment, this crack advances with a speed given by ref. 37

$$v_c = -\frac{da}{dt} \quad (3)$$

where $a = A/\Gamma$ is the contact radius. Examples of the variation of a with time are shown in Fig. 1B. We conducted an additional high-speed measurement series for retraction speeds of 10, 50, 250, and 500 $\mu\text{m s}^{-1}$, where force and contact area were synchronised and both recorded with 500 Hz. From these data, we determined that the peak detachment force P_{max} occurred when the contact area reached a critical value A_c at $30.83 \pm 6.03\%$ of its maximum value A_{max} (mean \pm s. e., $n = 11$), independent of retraction speed (linear mixed model, $F_{1,42} = 0.04$, $p = 0.82$, $n = 11$). The speed of crack propagation at P_{max} was measured as the slope of a least-square regression of $a(A_c)$ against time, including two data points on either side of $a(A_c)$.

In order to investigate whether detachment is directional, the peel velocity in the longitudinal and transverse directions was measured as the change in the length and width of the contact area, respectively, *via* a least-square regression of the filtered data against time, including two data points on either side of 60, 40 and 20% of A_{max} , respectively.

Modelling and statistics

The effects of retraction speed, accumulation/depletion and shear force on adhesion were analysed with linear mixed models using the R package *nlme*, v3.1–119. Ratios were arcsine-square root transformed prior to analysis to correct for the non-normality of residuals. Eqn (2) was fitted to the data as follows: v_c and P_{max} were averaged for each retraction speed. In order to estimate P_0 , we used independent force data, acquired with the same set-up and insects of a similar size, but at a slower retraction speed of $1 \mu\text{m s}^{-1}$. The measured crack speed and the corresponding peak

adhesive force were combined with the data measured at a retraction speed of $10 \mu\text{m s}^{-1}$ to linearly extrapolate the peak adhesive force under equilibrium conditions (*i.e.* $v_c = 0$), yielding $P_0 = 0.12 \text{ mN}$ as an upper limit of P_0 . The parameters n and v^* were fitted to the averaged data using a non-linear least squares algorithm.

The value of A_c used for the measurement of the speed of crack propagation depends on the pre-load and carries some uncertainty, but a speed-independent critical area has been reported before for flat punches made from polyurethane.⁴⁶ We repeated our analysis using values of A_c of 40% and 50% of A_{max} and found that the qualitative results remained unaffected.

Data reported in the text are mean \pm standard deviation unless otherwise stated. All statistical analysis was carried out with R v.3.0.3.⁵⁶

Results

Influence of retraction speed on adhesion and crack propagation speed

Despite a two hundred-fold variation in retraction speed, peak adhesion varied only moderately, by a factor of around three, from a minimum of $0.16 \pm 0.07 \text{ mN}$ measured at $10 \mu\text{m s}^{-1}$ retraction speed, to a peak value of 0.52 ± 0.21 observed at $2000 \mu\text{m s}^{-1}$ retraction speed (linear mixed model, $F_{1,95} = 72.67$, $p < 0.001$, $n = 16$; see Fig. 2A). Thus, the largest adhesion force was still less than 10% of the animals’ body weight. Crack propagation speed, in turn, increased more strongly with retraction speed, from a minimum of $9 \pm 3 \mu\text{m s}^{-1}$, up to a maximum of $1482 \pm 394 \mu\text{m s}^{-1}$ (linear mixed model, $F_{1,95} = 224.19$, $p < 0.001$, $n = 16$; see Fig. 2B).

Influence of retraction speed on the ‘mode of detachment’

The aspect ratio of the pads’ contact area (transverse width divided by distal–proximal length) remained constant during detachment, was independent of the applied retraction speed, and averaged 1.6 ± 0.33 ($n = 16$, see ESI† for detailed statistics). Accordingly, the ratio of the lateral and distal–proximal peeling velocities did not differ significantly from the aspect ratio (paired *t*-test, $t_{15} = -1.4$, $p = 0.18$, $n = 16$), and remained constant during detachment, again independent of the retraction speed (see ESI†). The width of the pads changed approximately 1.8 ± 0.6 faster than their distal–proximal length ($n = 16$). However, peeling from both left and right, and from distal and proximal, occurred with equal speed (left *vs.* right: paired *t*-test, $t_{15} = -1.24$, $p = 0.24$; distal *vs.* proximal: paired *t*-test, $t_{15} = -1.12$, $p = 0.28$, $n = 16$).

Influence of fluid depletion and accumulation on adhesion and crack propagation speed

The effect of retraction speed on adhesion did not differ between the ‘accumulated’ and the ‘depleted’ conditions (linear mixed model, $F_{1,523} = 2.93$, $p = 0.087$, $n = 10$, see Fig. 3), and was independent of the step number – a proxy for the amount of fluid depleted or accumulated ($F_{1,523} = 1.39$, $p = 0.24$, $n = 10$, see Fig. 3). Adhesion, however, varied significantly with step number



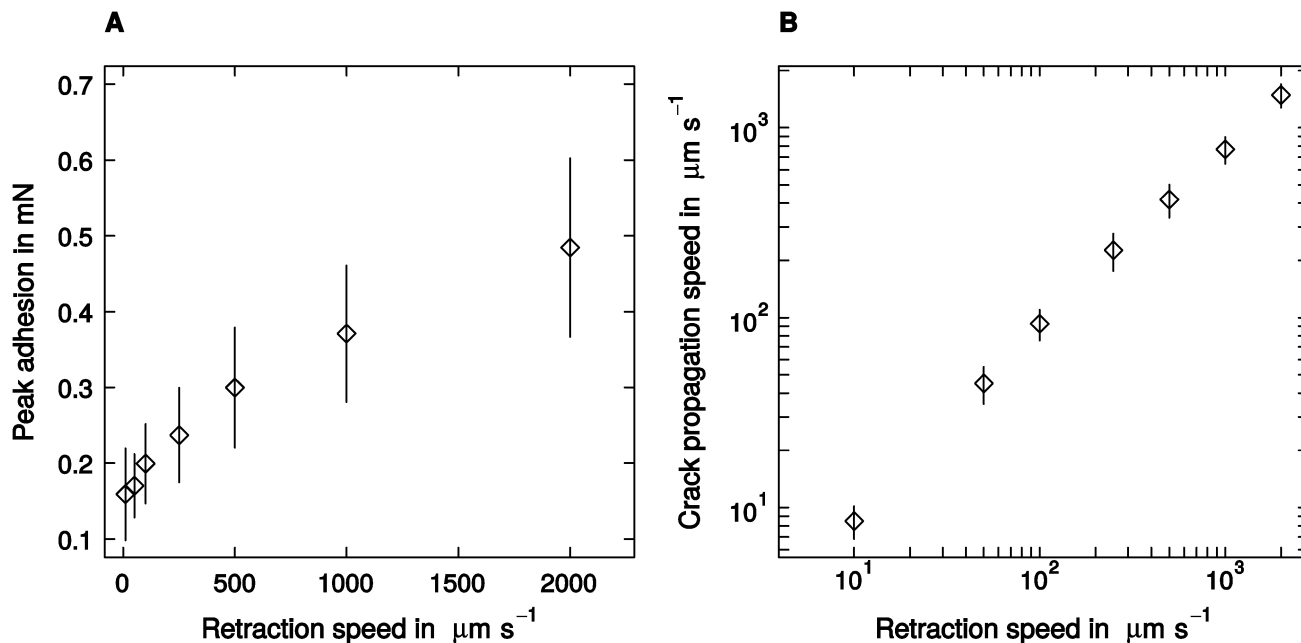


Fig. 2 (A) Adhesion of the attachment pads of *Carausius morosus* stick insects increased significantly with retraction speed. (B) The speed of crack propagation varied over three orders of magnitude (both $n = 16$). Error bars show 95% confidence intervals.

($F_{1,523} = 62.39$, $p < 0.001$, $n = 10$), but this effect was significantly different when fluid was depleted or accumulated ($F_{1,523} = 27.41$, $p < 0.001$, $n = 10$). Adhesion showed a small but insignificant trend to decrease with step number in the accumulated condition ($F_{1,258} = 1.54$, $p = 0.22$, $n = 10$). However, it increased

significantly when the pads were depleted ($F_{1,258} = 27.16$, $p < 0.001$, $n = 10$, see Fig. 3).

Crack propagation speed (measured for the first and the last step) did neither differ between the 'accumulated' and 'depleted' condition (linear mixed model, $F_{1,107} = 0.30$, $p = 0.58$, $n = 10$),

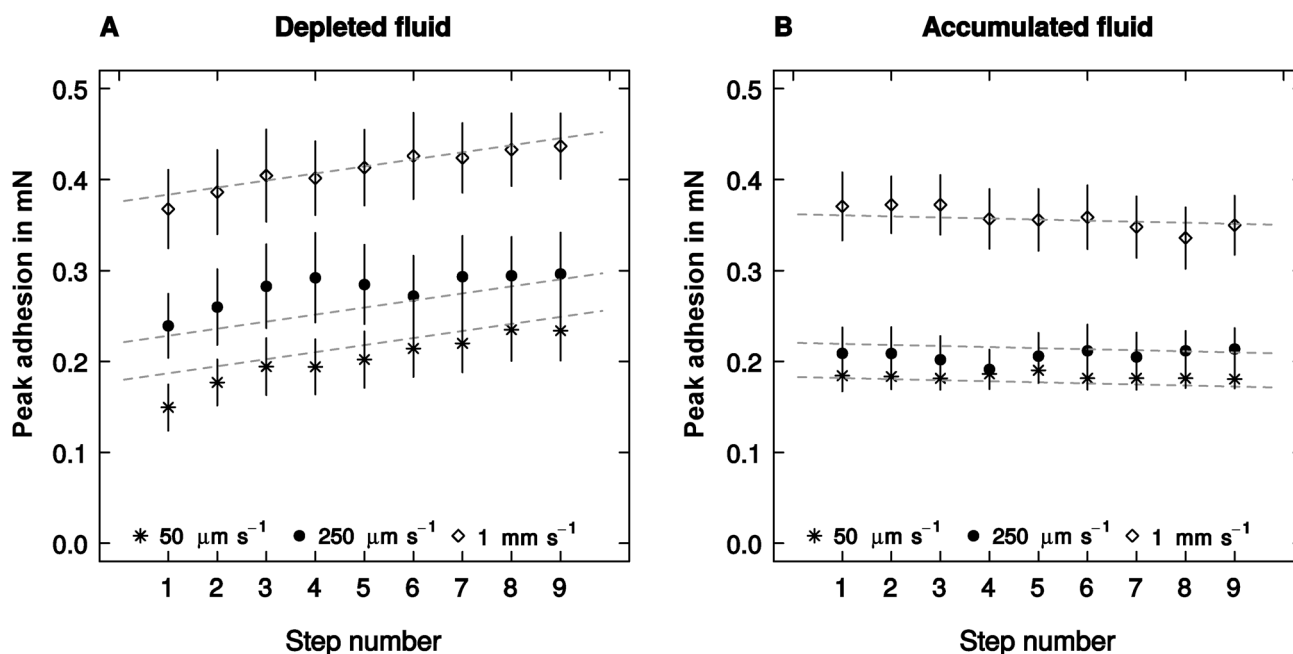


Fig. 3 The amount of secretion in the contact zone was experimentally varied by performing repeated artificial 'steps' on either 'fresh' spots ('depleted' – (A)) or repeatedly on the same spot ('accumulated', (B)). Adhesion of the attachment pads of *Carausius morosus* stick insects increased when secretion was depleted, but this effect was independent of retraction speed. When secretion was accumulated, the adhesive force showed a non-significant decreasing trend, again independent of the retraction speed (both $n = 10$). The lines are the result of a linear mixed model regression where the animals were a random factor, and step number and retraction speed were fixed factors. Error bars show the standard error of the mean.



nor between the first and last step ($F_{1,107} = 1.16$, $p = 0.28$, $n = 10$). Retraction speed was the only fixed factor exhibiting a significant influence on crack propagation speed, explaining around 93% of its variation ($F_{1,107} = 117.25$, $p < 0.001$, $n = 10$).

Influence of shear force on the relationship between adhesion and retraction speed

Both shear force and retraction speed exhibited a significant influence on adhesion (linear mixed model, shear force: $F_{1,87} = 328.37$,

$p < 0.001$; retraction speed: $F_{1,87} = 34.68$, $p < 0.001$, $n = 6$ for both). However, the effect of shear force was markedly larger (see Fig. 4), and independent of the retraction speed ($F_{1,87} = 0.007$, $p > 0.93$, $n = 6$). Adhesion varied by almost an order of magnitude, from around 0.26 ± 0.13 mN for detachments without a shear force, up to 2.15 ± 0.71 mN for detachments after the application of 4 mN shear force. These peak adhesive forces correspond to around a third of the animals' body weight. Despite the small range, shear force explained around 72% of the variation in adhesion. Retraction speed, in contrast, accounted for only 5% of the variation in adhesion (see Fig. 4).

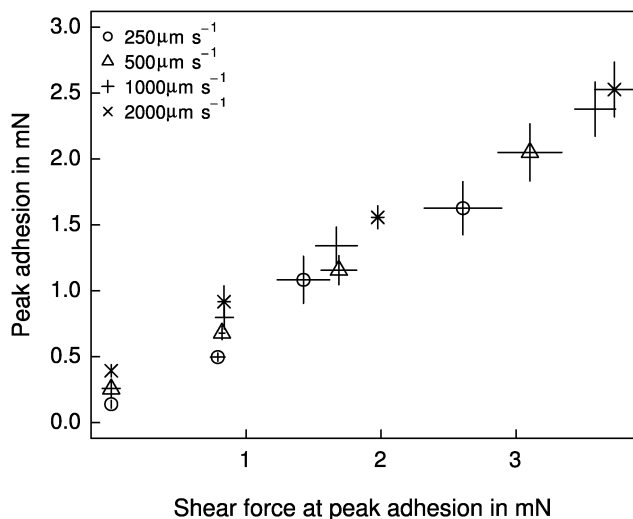


Fig. 4 Adhesion of the attachment pads of *Carausius morosus* was significantly influenced by both the retraction speed and the shear force acting during detachment, but the two effects were independent of each other, and the effect of shear force was markedly larger ($n = 6$). Error bars show the standard error of the mean.

Relationship between strain energy release rate and crack propagation speed

The relationship between relative energy dissipation $G/G_0 - 1$ and crack propagation speed is shown in Fig. 5, together with a fit of eqn (2), performed with the assumption that the adhesive pads resemble a flat punch, or a spherical indenter/thin adhesive tape, respectively. The model residuals were random, normally distributed, and the fits explained a significant amount of the variation of the energy dissipation with crack propagation speed (see Table 2).

The empirical constant n varied between 0.49 for the adhesive tape/spherical indenter, and 0.77 for the flat punch (95% confidence intervals (0.44, 0.55) and (0.68, 0.86), respectively, Fig. 5). The estimated amount of dissipated energy differed considerably between the models, which is reflected in different fitted values of v^* , the crack propagation speed at which G doubles compared to G_0 . For the adhesive tape/spherical indenter, v^* was fitted as $136 \mu\text{m s}^{-1}$, while it was $37 \mu\text{m s}^{-1}$ for the flat punch geometry (95% CI (109, 166) $\mu\text{m s}^{-1}$, and (24, 53) $\mu\text{m s}^{-1}$, respectively, Fig. 5).

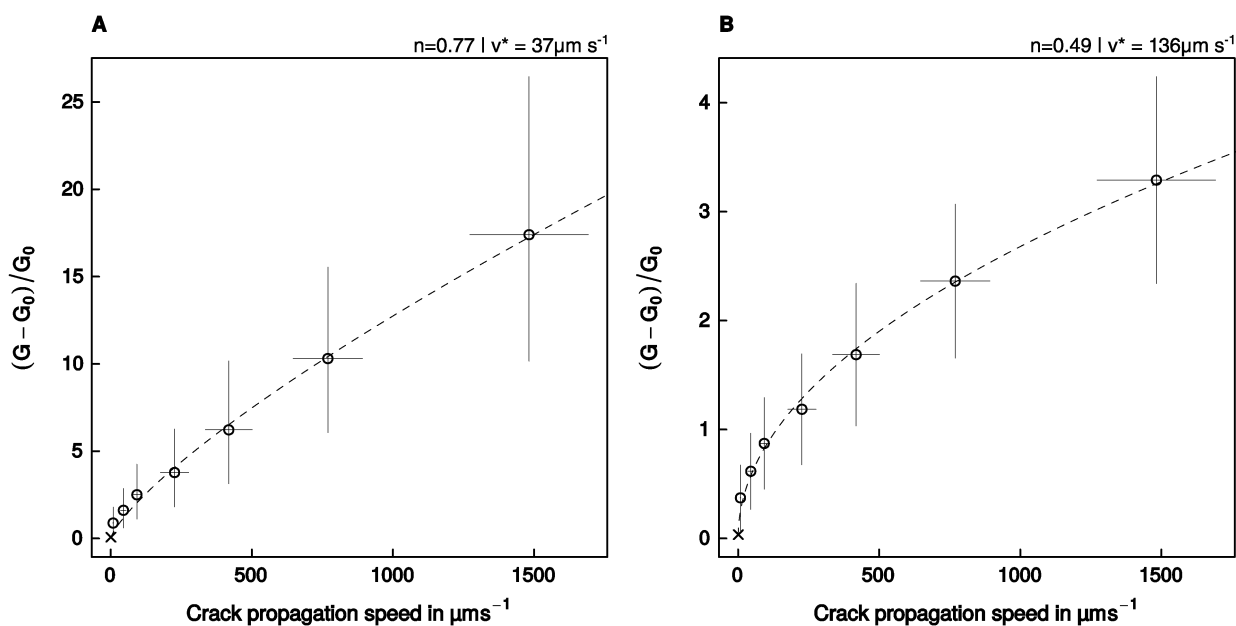


Fig. 5 An empirical power law relating the relative crack extension force to the speed of crack propagation (eqn (2)) was fitted to the experimental data assuming that the adhesive pads resemble (A) a flat punch, or (B) a thin stripe of adhesive tape/a spherical indenter. Error bars show the 95% confidence intervals around the mean. The crosses show the additional data point obtained at a retraction speed of $1 \mu\text{m s}^{-1}$, which was used to estimate P_0 , but was not included in the fit (see text for details).



Table 2 Summary of statistical tests for the normality and randomness of model residuals, along with the residual standard error (R. s. e.) of the model fit, corresponding to the fits shown in Fig. 5(A and B)

| Geometry | p (Shapiro–Wilk) | p (Runs-test) | R. s. e. |
|--------------------------------------|--------------------|-----------------|----------|
| Flat punch | 0.2 | 0.22 | 0.43 |
| Adhesive tape/ spherical indenter | 0.77 | 0.23 | 0.08 |

Discussion

Many insects are able to sustain detachment forces equivalent to multiple times their own body weight, yet they can attach and detach their feet effortlessly within milliseconds. Combining strong attachment with rapid detachment is a pre-requisite for dynamic adhesives used during locomotion, and a significant contribution of time-dependent viscous forces may be in conflict with these requirements. Our study revealed two key results concerning the role and origin of viscous dissipation during the detachment of ‘wet’ adhesive pads of stick insects. First, insect pads exhibited only a weak velocity-dependence – the increase of adhesive force with retraction speed was small relative to the animals’ body weight, and negligible compared to the effect of shear forces. Thus, viscous forces likely only play a minor role in the adhesion of ‘wet’ adhesive pads, and its modulation during locomotion. Second, the effect of retraction speed was independent of the amount of secretion present in the contact zone. Thus, the contribution of the secretion’s viscosity appears to be negligible. Instead, the velocity-dependence of adhesion may be explained by relating the critical strain energy release rate to the speed of crack propagation, and our data are in good agreement with a simple empirical power law of the form $G/G_0 - 1 \propto (v_c/v^*)^n$, commonly used to study the rate-dependence of ‘dry’ materials.

In the following discussion, we will first focus on the information implicit in the observed rate-dependence, specifically regarding the origin of the dissipation, the structural properties of the pad, and the mechanism of attachment. We will then combine these insights with data on the performance of ‘dry’ and ‘wet’ adhesives from previous publications to discuss the functional significance of the pad secretion.

Rate-dependence of insect pad adhesion

In this study, we used a well-established empirical model to relate the strain energy release rate to the speed of crack propagation. This relationship is determined by three empirical constants, G_0 , n and v^* , all of which contain some information about the adhesive interface, and the processes underlying energy dissipation during detachment.

The strength of the adhesive bonds: G_0 . G_0 is equal to the thermodynamic work of adhesion under true equilibrium conditions, and thus contains some information about the nature of the adhesive bonds that are broken during non-cohesive failure of the adhesive. We experimentally obtained an upper bound for P_0 , the force required to initiate crack propagation, and G_0 depends on the geometry and stiffness of the adhesive. For a flat punch, $G_0 = P_0^2/(6\pi a_{\text{crit}}^3 K)$, where $a_{\text{crit}} = 71.54 \mu\text{m}$ is

the contact radius at P_0 , and K is the reduced elastic modulus. Assuming that $K \approx 100 \text{ kPa}$,⁵⁷ $G_{0,\text{punch}} = 21 \text{ mJ m}^{-2}$. For an adhesive tape, $G_{0,\text{Tape}} = P_0/w = 180 \text{ mJ m}^{-2}$, where $w = 670 \mu\text{m}$ is the length of the peel line, which we approximated as the pad perimeter at P_0 . Lastly, for the sphere, $G_{0,\text{Sphere}} = 57 \text{ mJ m}^{-2}$ (see below). Thus $21 < G_0 < 180 \text{ mJ m}^{-2}$, similar to values reported for elastomers,^{36,37,41,43,44,58} and in excellent agreement with the expectation for weak, non-covalent bonds such as van-der-Waals forces ($\approx 50 \text{ mJ m}^{-2}$).

The adhesion of ‘wet’ biological pads is often attributed to capillary forces, while ‘dry’ pads are thought to rely on van-der-Waals forces. For a ‘dry’ sphere, $G_0 = 2/3P_0(\pi R)^{-1}$,⁴⁹ and for a ‘wet’ sphere, $\gamma = 1/3P_0(\pi R)^{-1}$,⁵⁹ where γ is the surface tension of the liquid which is assumed to completely wet the surface. Using $R = 450 \mu\text{m}$,[‡] and $P_0 = 0.12 \text{ mN}$ yields $G_0 = 57 \text{ mN m}^{-1}$, and $\gamma = 28 \text{ mN m}^{-1}$, both plausible values for interactions based on van-der-Waals forces or on the surface tension of an oily secretion. Thus, this simple quantitative argument does not yield decisive evidence for either of the two mechanisms.

The origin of the dissipation: n . Our experimental data followed a relationship of the form $G/G_0 - 1 \propto (v_c/v^*)^n$, where $0.49 < n < 0.77$, again in excellent agreement with values for soft elastomers where $n \approx 0.6$.^{36,37,41,43–46,60} Several authors have linked the power-law coefficient n to the dissipative processes close to the crack-tip,^{37,61,62} and one common approach is the use of Dugdale models.^{37,61} The principal idea here is to introduce a critical decay distance δ_c above which the adhesive interaction between the two separated materials plunges to zero, and below which it has a constant strength. The length of the ‘cohesive’ zone, where $\delta < \delta_c$, depends on the stiffness of the adhesive, which for viscoelastic materials is a function of the deformation frequency, providing the connection between crack propagation speed, viscoelasticity and the strain energy release rate. However, as we are not aware of any data on the frequency-dependence of the stiffness of stick insect pads, a further quantitative exploration of such models is currently infeasible.

Remarkably, these approaches often assume that the crack propagation in a soft, dissipative material occurs in the same fashion as in a stiff, glassy material. In a detailed study, Hui *et al.*⁶³ showed that for soft materials with an adhesive strength comparable to their elastic modulus, cracks ‘blunt’ instead of propagate (see also ref. 62). As a consequence, the material close to the crack tip experiences large strains, and the resulting stresses may exceed the yield strength of the material, eventually causing cohesive failure, and the propagation of the crack.⁶³ This dissipative process may involve fibrillation, cavity nucleation, as well as lateral and vertical crack growth, all of which are characteristic of the failure of soft, pressure-sensitive adhesives.^{64–66} Clearly, animals which make repeated use of their soft pads need to minimise plastic deformation, and it is an interesting question *how* exactly this can be achieved. Hui *et al.*⁶³ suggested that in materials with sufficiently large strain hardening, ‘micro-cracks’ can form. The highly stretched material

‡ A Birn-Jeffery, unpublished data.



close to the blunted region is much stiffer than the material far away from it, so that the stresses at the interface can become sufficient to decohere the materials. Stick insect pads have a specialised cuticle ultrastructure, where larger principal rods branch into progressively finer fibres closer to the surface membrane formed by the epicuticle,^{57,67,68} and the outermost layer appears to be considerably softer than the subjacent procuticle.⁵⁷ It is unclear how these features influence the stress distribution around the crack tip, in particular for blunted cracks and large strains, but in principle, it appears plausible that they will result in strain hardening. A gradual change in ultrastructure and material properties may represent a strategy to avoid cohesive failure of the soft adhesive pads, but further studies are required to corroborate this hypothesis.

The magnitude of dissipation: v^* . v^* is the crack speed at which G doubles compared to G_0 . Thus, small values of v^* indicate a strongly dissipative material. For stick insect pads, we found a lower bound $v^* > 37 \mu\text{m s}^{-1}$, more than two orders of magnitude larger than measurements for elastomers where v^* is in the range of 2–300 nm s⁻¹.^{37,41,42,45,46} This indicates that the velocity-dependence of stick insects pads is weak compared to that of elastomers. The magnitude of v^* depends on the molecular features of the adhesive, the substrate, and their interface.^{37,43,44} However, as v^* is a purely empirical parameter, we emphasize that the following arguments must be treated with caution.

First, v^* is inversely related to the relaxation time of the adhesive,⁴³ consistent with the interpretation that the rate-dependence is caused by a viscoelastic material response.³⁷ For rubbery materials, the relaxation time may vary between a few to several hundred seconds.⁴³ Gorb *et al.*²⁹ investigated the viscoelastic properties of the adhesive pads of a bush cricket, and reported a fast (≈ 0.6 s) and a slow (≈ 41 s) relaxation. Thus, the differences between the relaxation time of soft adhesive pads and common elastomers might be too small to fully explain the difference in energy dissipation. However, this conclusion remains speculative until reliable data for stick insect pads are available.

Second, v^* is related to the mobility of molecules at the interface.^{44,69,70} For rubbery materials on glass-like substrates, surface molecules may have little or no segmental mobility, resulting in sudden rupture of the bonds, and a considerable increase in G .⁴⁴ In the presence of thin interfacial layers with high segmental mobility, separation can occur in a more continuous manner, significantly decreasing adhesion and its velocity-dependence.^{44,69–71} Effectively, the interfacial film acts a ‘release layer’ through which the crack propagates, akin to a lubrication effect. We suggest that the thin lipid layer covering the adhesive pads may convey such a function, and thus decrease viscous dissipation during detachment. This interpretation can also account for the increase of adhesion when pads were ‘depleted’, and the trend for adhesion to decrease when footprints were ‘accumulated’. Repeated steps at the same position may lead to a contamination of the substrate with surface molecules, reducing the otherwise high surface energy of glass, and thus reducing G_0 . A similar effect has been

reported for ‘dry’ gecko pads (see Table 3), and for repeated adhesion measurements on polydimethylsiloxane surfaces.⁷² Continuously decreasing the amount of free molecules at the interface (‘depletion’), in turn, can reduce the screening of the direct adhesive interaction between the pad material and the surface, resulting in an increase in G_0 .⁴⁴

The mechanism of attachment in ‘wet’ adhesive pads

Previous authors have discussed a ‘wet adhesion model’ for adhesive pads of tree frogs and insects, where static capillary forces are combined with dynamic forces contributed by the fluid’s viscosity.^{4,16,20,25} Following this idea for a ‘wet’ sphere yields^{59,73}

$$F_{\text{wet}} = 3\pi R\gamma + 6\pi R^2\eta\frac{v}{h} \quad (4)$$

where η is the viscosity of the fluid, and h is the fluid film thickness underneath the centre of the sphere. Eqn (4) implies that if the static attachment force of insect pads is explained by capillary forces, the increase of dynamic (viscous) forces with retraction speed should depend on the amount of fluid in the contact zone, in contradiction with our experimental data (see Fig. 3). However, it has been shown that when liquid films are confined between elastic solids, elastic deformation of the solids can dominate the overall mechanical response.^{75,76} Such elasto-hydrodynamic effects become important for soft solids and strongly confined fluids. For an oscillating drainage flow between a sphere and a plane with frequency $\omega/2\pi$, it has been shown that the transition from the viscous flow to the elastic deformation regime occurs at a critical fluid film thickness of

$$h_c \approx R\left(\frac{\omega\eta}{K}\right)^{2/3} \quad (5)$$

where R is the pad’s radius of curvature and K is the reduced elastic modulus. Estimating $\omega \approx v/h_c$, $R \approx 450 \mu\text{m}$, $K \approx 100 \text{ kPa}$,⁵⁷ $\eta \approx 100 \text{ mPa s}$,^{21,27,28} and $v_1 = 50 \mu\text{m s}^{-1}$, a critical thickness of $0.8 \mu\text{m}$ is obtained. Even at this small velocity, the critical fluid thickness exceeds available estimates of the adhesive fluid thickness in the contact zone ($<100 \text{ nm}$),^{7–9,21,26,53,77,78} indicating that the insect adhesive pad is in ‘elastic confinement’. In this regime, the fluid secretion is ‘clamped’ by its viscosity, and the mechanical response will be dominated by the pad’s elastic deformation, as for a ‘dry’ pad. Thus, the secretion within the contact zone will not contribute to the adhesive force as suggested by eqn (5), but instead energy is mostly dissipated within the ‘bulk’ pad cuticle. However, the pad secretion will still influence adhesion in the crack tip, by giving the interface a higher mobility (see above).

The ‘dry’ model (eqn (2)) also has a rate-independent (G_0) and a rate-dependent ($G_0(v_c/v^*)^2$) term. We found that the adhesive forces measured at low and high retraction speeds during ‘depletion’ differed by a factor of 3.47 (95% CI 1.39–5.54) for the first step and by a factor of 2.2 (95% CI 1.44–2.95) for the last step. For the ‘dry’ model, the ratio between the adhesive forces measured at different retraction speeds should be

§ Here, we assumed that h is small compared to the total height of the meniscus, *i.e.* the sphere is very close to the surface.⁷⁴



Table 3 Comparison of performance of 'dry' and 'wet' biological adhesives

| Experimental | Result | Shown for... | | Consistent with... | | Note |
|---|--|---|--|--------------------|---------------|--|
| | | 'dry' pads | 'wet' pads | 'dry' contact | 'Wet' contact | |
| Attachment performance at different sliding/detachment speeds | Forces increase with rate | Geckos ^{30,32,102} | Tree frogs, ²⁰ ants, ^{21,23} stick insects ⁵² | Yes | Yes | For insects, the rate-dependence of adhesion and friction is quantitatively inconsistent with a continuous liquid film in the pad contact zone, see text. |
| Attachment performance at different temperatures | Decreases with temperature | Geckos ¹⁰³ | Cockroaches, ¹⁷ ants ^{21,23} | Yes | Yes | For ants, only dynamic forces were temperature-dependent. |
| Attachment performance at different relative humidities | Is significantly affected | Geckos ^{30,93,104} | Spiders, ¹⁰⁵ beetles, ⁵¹ no effect in stick insects ⁵² | Yes | Yes | In most cases, attachment forces increased with humidity. |
| Treat pads with solvents/alcohol | Attachment performance is reduced | Geckos ^a | Bugs, ¹⁸ flies ⁸ | ? | Yes | Influence on stiffness? |
| Attachment performance on surfaces flooded with water | Is significantly affected | Geckos ¹⁰⁶ | Tree frogs, ^{4,95} ants ¹⁰⁷ | Yes | Yes | Effect depends on the surface energies of the involved materials. |
| Attachment performance on smooth surfaces with different normal (pre-)loads | No significant effect for adhesive pads | Geckos ¹⁰⁸ | Stick insects, ^{50,52,109} beetles ¹⁰⁹ | Yes | ? | The range of loads was small, and effects were found when fluid was accumulated. ⁵² |
| Adhesion dependent on shear force applied during detachment | Increases when pulled, decreases when pushed | Geckos ^{94,100} | Stick insects, ⁵⁰ beetles & cockroaches, ⁸¹ tree frogs ⁹⁵ | Yes | ? | For geckos, it is still unclear whether the relationship is independent of contact area. |
| Contact time before detachment | Adhesion increases with contact time | — | Stick insects ¹¹⁰ | Yes | Yes | |
| Test for static friction | Present, smaller than dynamic friction | Chameleons, ¹¹¹ geckos ¹³ | Ants, ^{21,23} stick insects, ⁵² tree frogs, ²⁴ spiders ¹³ | ? | ? | The transition to sliding is significantly altered if 'dry' materials are microstructured. ^{112,113} For 'wet' hairy pads, surface tension may give rise to considerable static shear stress even for Newtonian fluids. ⁸¹ |
| Perform repeated slides on the same position | Friction and adhesion decrease | Geckos ^a | Stick insects, ^{52,109} beetles ¹⁰⁹ | ? | Yes | Soft, 'rubbery' polymers have been shown to leave residues behind, affecting their adhesive performance in repeated trials on the same spot. ⁷² |
| Perform repeated slides/pull-offs on new positions with high frequency | Friction and adhesion increase | Geckos ^b | Stick insects, ^{52,109} beetles ¹⁰⁹ | ? | Yes | The effect is reversed when experiments are performed on a rough surface. ⁵² |
| Attachment performance on substrates with different surface energy | Mixed reports, but generally small or no effects | Geckos ^{106,114} | Tree frogs, ⁴ beetles, ^{11,115–119} aphids, ¹⁹ cockroaches ¹²⁰ | ? | ? | A comparison to theoretical predictions requires the estimation of unknown parameters, and the use of simplified models. |
| Attachment performance after pad contamination | Pads lose & then regain attachment ability | Geckos ¹²¹ | Beetles & stick insects, ¹²² tree frogs ¹²³ | — | — | Recovery rates appear to be higher for 'wet' pads. ¹²² |

^a K Autumn, pers. communication. ^b 25% increase in adhesion, 5% decrease in friction.¹⁰²

independent of fluid depletion ('step number'). The mean crack propagation speeds measured during the depletion experiments, $v_{c,1000} = 676 \mu\text{m s}^{-1}$ and $v_{c,50} = 47 \mu\text{m s}^{-1}$, as well as $v^* = 136 \mu\text{m s}^{-1}$ and $n = 0.49$, yield a ratio of $\kappa = P(v_{c,1000})/P(v_{c,50}) \approx 2$ between the forces measured at a retraction speed of 1000 and $50 \mu\text{m s}^{-1}$,

not significantly different from the ratios observed for the first and the last step (t -test, $t_9 = 1.5$, $p = 0.16$ and $t_9 = 0.35$, $p = 0.73$, respectively). Thus, the rate-dependent contribution predicted by the fracture mechanics model is small enough to be consistent with the absence of a measurable interaction.



Remarkably, modelling 'wet' adhesive pads as 'dry' elastomers can also account for the shear stress generated by insect pads, which is at least one order of magnitude too large to be explained by hydrodynamic lubrication.^{21,23,52,79,80} Friction of soft materials is dominated by adhesive forces,⁸¹ and their contribution to the shear stress σ can be linked to the difference between the energy required to break and form interfacial bonds (corresponding to an advancing or a receding crack), G_A and G_R , respectively.^{82,83} G_R is approximately G_0 , while G_A depends on the crack propagation speed. Eqn (2) yields

$$\sigma \approx \frac{1}{\chi} G_0 \left(\frac{v}{v^*} \right)^n \quad (6)$$

where $v \approx v_c$ is the sliding speed, and χ is a characteristic length scale representing the distance between bonds that are repeatedly broken and reformed during sliding.^{82–84} For sliding speeds between 0.1–1 $\mu\text{m s}^{-1}$, stick insect pads show a shear stress between 80–100 kPa.⁸⁰ Using $v = 0.1 \mu\text{m s}^{-1}$, $v^* = 136 \mu\text{m s}^{-1}$, $n = 0.49$, $\sigma = 80 \text{ kPa}$, and $G_0 = 0.05 \text{ J m}^{-2}$, yields $\chi \approx 18 \text{ nm}$, consistent with the friction of soft, 'dry' elastomers, where $\chi \approx 1\text{--}10 \text{ nm}$ is of a molecular dimension.^{82–85} Eqn (6) may also help to understand why the friction force generated by biological adhesive pads is considerably larger than their adhesion. Both adhesion and friction depend on the strain energy release rate which is of dimension force per length. However, two important differences exist: first, the two characteristic lengths determining net adhesion and friction, respectively, are quite different. For friction, the length is A/χ , where A is the contact area. For adhesion, in turn, the length is a characteristic dimension of the contact area, for example its width or radius (assuming length scaling). For stick insects, these lengths differ by around four orders of magnitude. Second, friction is caused by the difference in the energy required to form vs. to break adhesive bonds $G_A - G_R$, and thus for $v_c \ll v^*$, $(G_A - G_R)/G_R \propto (v_c/v^*)^n$. Together, these effects can cause large differences in the magnitude of friction and adhesion: for stick insect pads sliding at a speed of 1 $\mu\text{m s}^{-1}$, friction is approximately 100 times larger than the adhesion measured in the absence of shear forces.

The previous discussion suggests that the rate-dependence of 'wet' adhesive pads is akin to that of 'dry' elastomers, and our data are consistent with a simple model based on fracture mechanics. Fracture mechanics provide a simple yet powerful theoretical framework for the quantitative study of biological adhesives, and can explain a number of performance characteristics of insect pads which are quantitatively inconsistent with simple predictions for 'wet' adhesive contacts. Thus, the secretion does not appear to behave like a Newtonian 'bulk' fluid,^{21,52,80} and indeed it has been argued that it may be 'semi-solid' at ambient temperatures.⁸⁶ Based on these observations, we suggest that the viscosity of the pad secretion does not contribute significantly to adhesion and friction forces in insects. Instead, stick insects may attach *via* weak non-covalent forces between the pad and the surface, as is the case for the 'dry' adhesive pads of geckos. What, then, is the functional significance of the secretion, and how

does the performance of 'wet' pads differ from that of 'dry' biological pads?

The function of the fluid and the difference between 'wet' and 'dry' biological adhesives

We investigated functional differences between 'wet' and 'dry' adhesive systems by conducting a literature survey summarising experimental treatments and their impact on the pads' performance (Table 3). The summary clearly shows that the performance of 'wet' and 'dry' adhesive systems is strikingly similar. Nevertheless, the published interpretations of these findings often invoked explanations specific to 'wet' or 'dry' contacts. For example, Emerson and Diehl⁴ observed that the adhesive performance of tree frogs on glass decreased significantly when the pads were immersed in water, and concluded that attachment is aided by capillary forces. However, a significant reduction in attachment performance has also been reported for the friction of 'dry' gecko pads on hydrophilic surfaces immersed in water.⁸⁷ Given that dynamic biological attachment pads face similar functional requirements, it comes as no surprise that similar experimental treatments have similar effects. However, the implication of this finding is that it is surprisingly hard, if not impossible, to draw reliable conclusions on the physical mechanisms underlying attachment from such experiments, at least if they are not conducted in a rigorous comparative manner. The key problem is that the attachment performance of soft, rubbery materials has similar characteristics as that of 'wet' contacts. Thus far, we are not aware of a single experiment which has yielded a qualitatively different result for 'dry' vs. 'wet' adhesive pads. Clearly, the physical attachment mechanisms of both types of pads are either identical, or cannot be distinguished with the available information.

However, this conclusion does not preclude a functional importance of the pad secretion as such. For example, the pad secretion may help to fill in small gaps on rough surfaces, thereby increasing contact area and thus adhesion.⁵² Other experiments revealed a significant drop in attachment performance when pads were washed with solvents, likely resulting in a removal of the secretion (see Table 3). Notably, the entire body of insects is covered with a thin lipid layer, and comparative analyses between the pad secretion and samples taken from the other parts of the insects' body have not revealed any significant qualitative differences in chemical composition.^{79,86,88–90} It appears plausible that this chemical congruence implies that the lipid secretion has a similar function in the pads as in the rest of the body.¹⁴ The key function of the whole-body lipid coverage is to avoid evaporation, a crucial issue for small animals with large surface-to-volume ratios, and removal of the lipid layer likely compromises this protective function. The subsequent reduction of the water content of the soft pad cuticle likely increases its stiffness,^{91,92} providing a possible explanation for the observed drop in performance. Strikingly, geckos may face a similar problem, as the stiffness of β -keratin is also controlled by hydration.⁹³

Our results suggest that another function of the secretion may be to serve as a lubricating separation layer, reducing adhesion



and in particular its rate-dependence. An adaptation that serves to reduce adhesion may be explained by the functional requirement to combine strong attachment with rapid and effortless detachment. There is ample evidence that adhesion is controlled *via* shear forces, in 'dry', 'wet', 'hairy' and 'smooth' systems,^{50,81,94,95} but the details of this mechanism remain unclear. Our results clearly show that shear forces exhibit a much larger effect on adhesion than retraction speed, and thus are likely the main tool for the modulation of surface attachment during locomotion.⁸¹ Thus, attachment forces in the absence of shear can or even should be negligible to allow effortless detachment. Interestingly, a highly mobile interfacial layer may help to decrease attachment forces during purely normal separation, but may increase attachment forces *via* interfacial slippage when pads are simultaneously sheared.^{96–99} Gravish *et al.*¹⁰⁰ suggested that the shear-sensitivity of gecko pads is caused by significant energy dissipation *via* frictional sliding, and in insects, the presence of a thin interfacial layer may help to ensure that interfacial slippage occurs before the stress concentrations close to the crack tip are sufficient to advance the crack when pads are pulled off and sheared simultaneously. Remarkably, gecko pads leave tiny amounts of phospholipid 'footprints',¹⁰¹ which might also function as a lubricating separation layer as in arthropods. Clearly, comparative studies on the presence and role of thin lipid layers for the material properties and shear-sensitivity of adhesive pads in geckos, insects, and spiders are required to study the above mechanisms in more detail, and to improve our understanding of the design and function of biological adhesive pads.

Acknowledgements

D.L. thanks U. Abusomwan for pointing out some helpful literature. Both authors are grateful to M.Y. Strücker for her help with the synchronised force measurements, and the recordings at a retraction speed of $1 \mu\text{m s}^{-1}$. Two anonymous reviewers helped to improve this manuscript with their suggestions. This study was supported by research grants from the Cusanuswerk (to D.L.), as well as the Biotechnology and Biological Sciences Research Council (BB/I008667/1) and the Human Frontier Science Programme (RGP0034/2012) to W.F.

References

- J. Gillett and V. Wigglesworth, *Proc. R. Soc. B*, 1932, **111**, 364–376.
- M. D. Kendall, *Z. Zellforsch. Mikrosk. Anat.*, 1970, **109**, 112–137.
- V. V. Ernst, *Tissue Cell*, 1973, **5**, 97–104.
- S. Emerson and D. Diehl, *Biol. J. Linn. Soc.*, 1980, **13**, 199–216.
- A. Ghazi-Bayat and I. Hasenfuss, *Zool. Anz.*, 1980, **204**, 13–18.
- D. M. Green, *Copeia*, 1981, **1981**, 790–796.
- N. Stork, *J. Nat. Hist.*, 1983, **17**, 583–597.
- G. Walker, A. B. Yulf and J. Ratcliffe, *J. Zool.*, 1985, **205**, 297–307.
- A. D. Lees and J. Hardie, *J. Exp. Biol.*, 1988, **136**, 209–228.
- S. Gorb, *Proc. R. Soc. London*, 1998, **265**, 747–752.
- T. Eisner and D. Aneshansley, *Proc. Natl. Acad. Sci. U. S. A.*, 2000, **97**, 6568–6573.
- J. M. Smith, J. W. Barnes, J. Downie and G. Ruxton, *J. Zool.*, 2006, **270**, 372–383.
- A. M. Peattie, J.-H. Dirks, S. Henriques and W. Federle, *PLoS One*, 2011, **6**, e20485.
- O. Betz, *Biological Adhesive Systems*, Springer, 2010, pp. 111–152.
- J.-H. Dirks and W. Federle, *Soft Matter*, 2011, **7**, 11047–11053.
- J.-H. Dirks, *Beilstein J. Nanotechnol.*, 2014, **5**, 1160–1166.
- L. Roth and E. Willis, *J. Exp. Zool.*, 1952, **119**, 483–517.
- J. Edwards and M. Tarkanian, *Proc. R. Entomol. Soc.*, 1970, **45**, 1–5.
- A. F. G. Dixon, P. Croghan and R. Gowing, *J. Exp. Biol.*, 1990, **152**, 243–253.
- G. Hanna and J. W. Barnes, *J. Exp. Biol.*, 1991, **155**, 103–125.
- W. Federle, M. Riehle, A. S. Curtis and R. Full, *Integr. Comp. Biol.*, 2002, **42**, 1100–1106.
- W. Vötsch, G. Nicholson, R. Müller, Y. D. Stierhof, S. Gorb and U. Schwarz, *Insect Biochem. Mol. Biol.*, 2002, **32**, 1605–1613.
- W. Federle, W. Baumgartner and B. Hölldobler, *J. Exp. Biol.*, 2004, **206**, 67–74.
- W. Federle, J. W. Barnes, W. Baumgartner, P. Drechsler and J. M. Smith, *J. R. Soc., Interface*, 2006, **3**, 689–697.
- J. W. Barnes, *MRS Bull.*, 2007, **32**, 479–485.
- S. F. Geiselhardt, W. Federle, B. Prüm, S. Geiselhardt, S. Lamm and K. Peschke, *J. Insect Physiol.*, 2009, **56**, 398–404.
- B. Abou, C. Gay, B. Laurent, O. Cardoso, D. Voigt, H. Peisker and S. Gorb, *J. R. Soc., Interface*, 2010, **7**, 1745–1752.
- H. Peisker, L. Heepe, A. E. Kovalev and S. N. Gorb, *J. R. Soc., Interface*, 2014, **11**, 20140752.
- S. Gorb, Y. Jiao and M. Scherge, *J. Comp. Physiol., A*, 2000, **186**, 821–831.
- J. Puthoff, M. Prowse, M. Wilkinson and K. Autumn, *J. Exp. Biol.*, 2010, **213**, 3699–3704.
- J. W. Barnes, P. Goodwyn, M. Nokhbatolfoghahai and S. Gorb, *J. Comp. Physiol., A*, 2011, **197**, 969–978.
- J. Puthoff, M. Holbrook, M. Wilkinson, K. Jin, N. Pesika and K. Autumn, *Soft Matter*, 2013, **9**, 4855–4863.
- C. Gay, *Int. Comp. Biol.*, 2002, **42**, 1123–1126.
- C. Creton and P. Fabre, *Adhesion science and engineering*, Elsevier, Amsterdam, 2002, vol. 1, pp. 535–576.
- C. Creton, *MRS Bull.*, 2003, **28**, 434–439.
- M. Barquins and D. Maugis, *J. Adhes.*, 1981, **13**, 53–65.
- K. R. Shull, *Mat. Sci. Eng., R*, 2002, **36**, 1–45.
- H. Müller and W. G. Knauss, *J. Appl. Mech.*, 1971, **38**, 483–488.
- A. Gent and J. Schultz, *J. Adhes.*, 1972, **3**, 281–294.
- E. H. Andrews and A. J. Kinloch, *Proc. R. Soc. London, Ser. A*, 1973, **332**, 385–399.
- D. Maugis and M. Barquins, *J. Phys. D: Appl. Phys.*, 1978, **11**, 1989–2023.
- A. Gent, *Langmuir*, 1996, **12**, 4492–4496.
- D. Ahn and K. R. Shull, *Langmuir*, 1998, **14**, 3637–3645.



- 44 D. Ahn and K. R. Shull, *Langmuir*, 1998, **14**, 3646–3654.
- 45 A. J. Crosby and K. R. Shull, *J. Polym. Sci., Part B: Polym. Phys.*, 1999, **37**, 3455–3472.
- 46 U. Abusomwan and M. Sitti, *Appl. Phys. Lett.*, 2012, **101**, 211907.
- 47 K. Kendall, *J. Phys. D: Appl. Phys.*, 1971, **4**, 1186–1195.
- 48 R. Rivlin, *Paint Technol.*, 1944, **9**, 215–216.
- 49 K. Johnson, K. Kendall and A. Roberts, *Proc. R. Soc. London, Ser. A*, 1971, **324**, 301–313.
- 50 D. Labonte and W. Federle, *PLoS One*, 2013, **8**, e81943.
- 51 D. Voigt, J. Schuppert, S. Dattinger and S. Gorb, *J. Zool.*, 2010, **281**, 227–231.
- 52 P. Drechsler and W. Federle, *J. Comp. Physiol., A*, 2006, **192**, 1213–1222.
- 53 J.-H. Dirks and W. Federle, *J. R. Soc., Interface*, 2011, **8**, 952–960.
- 54 J. Schindelin, I. Arganda-Carreras, E. Frise, V. Kaynig, M. Longair, T. Pietzsch, S. Preibisch, C. Rueden, S. Saalfeld and B. Schmid, *Nat. Methods*, 2012, **9**, 676–682.
- 55 L. Huang and M. Wang, *Pattern Recognit.*, 1995, **28**, 41–51.
- 56 R Development Core Team, *R: A Language and Environment for Statistical Computing*, R Foundation for Statistical Computing, Vienna, Austria, 2013.
- 57 I. Scholz, W. Baumgartner and W. Federle, *J. Comp. Physiol., A*, 2008, **194**, 373–384.
- 58 B. Lorenz, B. Krick, N. Mulakaluri, M. Smolyakova, S. Dieluweit, W. Sawyer and B. Persson, *J. Phys.: Condens. Matter*, 2013, **25**, 225004.
- 59 A. Fogden and L. R. White, *J. Colloid Interface Sci.*, 1990, **138**, 414–430.
- 60 X. Feng, M. A. Meitl, A. M. Bowen, Y. Huang, R. G. Nuzzo and J. A. Rogers, *Langmuir*, 2007, **23**, 12555–12560.
- 61 J. Greenwood and K. Johnson, *Philos. Mag.*, 1981, **43**, 697–711.
- 62 B. Persson and E. Brener, *Phys. Rev. E: Stat., Nonlinear, Soft Matter Phys.*, 2005, **71**, 036123.
- 63 C.-Y. Hui, A. Jagota, S. Bennison and J. Londono, *Proc. R. Soc. London, Ser. A*, 2003, **459**, 1489–1516.
- 64 C. Creton and H. Lakrout, *J. Polym. Sci., Part B: Polym. Phys.*, 2000, **38**, 965–979.
- 65 A. J. Crosby, K. R. Shull, H. Lakrout and C. Creton, *J. Appl. Phys.*, 2000, **88**, 2956–2966.
- 66 C. Creton, J. Hooker and K. R. Shull, *Langmuir*, 2001, **17**, 4948–4954.
- 67 M. Bennemann, I. Scholz and W. Baumgartner, *Bioinspiration, Biomimetics, and Bioreplication, an Diego*, California, USA, 2011, p. 79751A-8.
- 68 M. Bennemann, S. Backhaus, I. Scholz, D. Park, J. Mayer and W. Baumgartner, *J. Exp. Biol.*, 2014, **217**, 3677–3687.
- 69 D. Ahn and K. R. Shull, *Macromolecules*, 1996, **29**, 4381–4390.
- 70 K. R. Shull, D. Ahn, W.-L. Chen, C. M. Flanigan and A. J. Crosby, *Macromol. Chem. Phys.*, 1998, **199**, 489–511.
- 71 F. D. Blum, B. C. Gandhi, D. Forciniti and L. R. Dharani, *Macromolecules*, 2005, **38**, 481–487.
- 72 E. Kroner, R. Maboudian and E. Arzt, *Adv. Eng. Mater.*, 2010, **12**, 398–404.
- 73 B. Francis and R. G. Horn, *J. Appl. Phys.*, 2001, **89**, 4167–4174.
- 74 S. Cai and B. Bhushan, *Mater. Sci. Eng., R*, 2008, **61**, 78–106.
- 75 S. Leroy and E. Charlaix, *J. Fluid Mech.*, 2011, **674**, 389–407.
- 76 R. Villey, E. Martinot, C. Cottin-Bizonne, M. Phaner-Goutorbe, L. Léger, F. Restagno and E. Charlaix, *Phys. Rev. Lett.*, 2013, **111**, 215701.
- 77 N. Stork, *Antenna*, 1983, **7**, 20–23.
- 78 W. Federle, *J. Exp. Biol.*, 2006, **209**, 2611–2621.
- 79 S. F. Geiselhardt, S. Geiselhardt and K. Peschke, *Chemoecology*, 2009, **19**, 185–193.
- 80 J. Dirks, C. Clemente and W. Federle, *J. R. Soc., Interface*, 2010, **7**, 587–593.
- 81 D. Labonte and W. Federle, *Philos. Trans. R. Soc., B*, 2015, **370**, 20140027.
- 82 H. Yoshizawa, Y. L. Chen and J. Israelachvili, *J. Phys. Chem.*, 1993, **97**, 4128–4140.
- 83 M. Heuberger, G. Luengo and J. Israelachvili, *J. Phys. Chem. B*, 1999, **103**, 10127–10135.
- 84 N. Chen, N. Maeda, M. Tirrell and J. Israelachvili, *Macromolecules*, 2005, **38**, 3491–3503.
- 85 K. Grosch, *Proc. R. Soc. London, Ser. A*, 1963, **274**, 21–39.
- 86 M. Reitz, H. Gerhardt, C. Schmitt, O. Betz, K. Albert and M. Lämmerhofer, *Anal. Chim. Acta*, 2015, **854**, 47–60.
- 87 A. Y. Stark, T. W. Sullivan and P. H. Niewiarowski, *J. Exp. Biol.*, 2012, **215**, 3080–3086.
- 88 A. Kosaki and R. Yamaoka, *Jpn. J. Appl. Entomol. Zool.*, 1996, **40**, 47–53.
- 89 O. Betz, *J. Morphol.*, 2003, **255**, 24–43.
- 90 S. Geiselhardt, S. Geiselhardt and K. Peschke, *Chemoecology*, 2011, **21**, 181–186.
- 91 J. F. Vincent and U. G. Wegst, *Arthropod Struct. Dev.*, 2004, **33**, 187–199.
- 92 D. Klocke and H. Schmitz, *Acta Biomater.*, 2011, **7**, 2935–2942.
- 93 M. Prowse, M. Wilkinson, J. Puthoff, G. Mayer and K. Autumn, *Acta Biomater.*, 2011, **7**, 733–738.
- 94 K. Autumn, A. Dittmore, D. Santos, M. Spenko and M. Cutkosky, *J. Exp. Biol.*, 2006, **209**, 3569–3579.
- 95 T. Endlein, A. Ji, D. Samuel, N. Yao, Z. Wang, W. J. P. Barnes, W. Federle, M. Kappl and Z. Dai, *J. R. Soc., Interface*, 2013, **10**, 20120838.
- 96 B. Newby, M. Chaudhury and H. Brown, *Science*, 1995, **269**, 1407–1409.
- 97 B. Newby and M. Chaudhury, *Langmuir*, 1998, **14**, 4865–4872.
- 98 A. Ghatak, K. Vorvolakos, H. She, D. L. Malotky and M. K. Chaudhury, *J. Phys. Chem. B*, 2000, **104**, 4018–4030.
- 99 R. R. Collino, N. R. Phillips, M. N. Rossol, R. M. McMeeking and M. R. Begley, *J. R. Soc., Interface*, 2014, **11**, 20140453.
- 100 N. Gravish, M. Wilkinson and K. Autumn, *J. R. Soc., Interface*, 2008, **5**, 339–348.
- 101 P. Y. Hsu, L. Ge, X. Li, A. Y. Stark, C. Wesdemiotis, P. H. Niewiarowski and A. Dhinojwala, *J. R. Soc., Interface*, 2011, **9**, 657–664.
- 102 N. Gravish, M. Wilkinson, S. Sponberg, A. Parness, N. Esparza, D. Soto, T. Yamaguchi, M. Broide, M. Cutkosky, C. Creton and K. Autumn, *J. R. Soc., Interface*, 2010, **7**, 259–269.



- 103 P. H. Niewiarowski, S. Lopez, L. Ge, E. Hagan and A. Dhinojwala, *PLoS One*, 2008, **3**, e2192.
- 104 G. Huber, H. Mantz, R. Spolenak, K. Mecke, K. Jacobs, S. N. Gorb and E. Arzt, *Proc. Natl. Acad. Sci. U. S. A.*, 2005, **102**, 16293–16296.
- 105 J. O. Wolff and S. N. Gorb, *Proc. R. Soc. B*, 2011, **279**, 139–143.
- 106 A. Y. Stark, I. Badge, N. A. Wucinich, T. W. Sullivan, P. H. Niewiarowski and A. Dhinojwala, *Proc. Natl. Acad. Sci. U. S. A.*, 2013, **110**, 6340–6345.
- 107 M. Scharmann, MSc thesis, Julius-Maximilians-Universität Würzburg, 2011.
- 108 K. Autumn, Y. Liang, S. Hsieh, W. Zesch, W. Chan, T. Kenny, R. Fearing and R. Full, *Nature*, 2000, **405**, 681–685.
- 109 J. M. R. Bullock, P. Drechsler and W. Federle, *J. Exp. Biol.*, 2008, **211**, 3333–3343.
- 110 P. Drechsler, PhD thesis, Julius-Maximilians-Universität Würzburg, 2008.
- 111 M. Spinner, G. Westhoff and S. N. Gorb, *Sci. Rep.*, 2014, **4**, 5481.
- 112 M. Varenberg and S. N. Gorb, *Adv. Mater.*, 2009, **21**, 483–486.
- 113 B. Lorenz and B. Persson, *J. Phys.: Condens. Matter*, 2012, **24**, 225008.
- 114 K. Autumn, M. Sitti, Y. A. Liang, A. M. Peattie, W. R. Hansen, S. Sponberg, T. W. Kenny, R. Fearing, J. N. Israelachvili and R. J. Full, *Proc. Natl. Acad. Sci. U. S. A.*, 2002, **99**, 12252–12256.
- 115 N. Stork, *Zool. J. Linn. Soc.*, 1980, **68**, 173–306.
- 116 S. N. Gorb, R. G. Beutel, E. V. Gorb, Y. Jiao, V. Kastner, S. Niederegger, V. L. Popov, M. Scherge, U. Schwarz and W. Vötsch, *Integr. Comp. Biol.*, 2002, **42**, 1127–1139.
- 117 E. Gorb and S. Gorb, *Entomol. Exp. Appl.*, 2009, **130**, 222–228.
- 118 J. M. R. Bullock, PhD thesis, University of Cambridge, 2010.
- 119 B. Prüm, H. Florian Bohn, R. Seidel, S. Rubach and T. Speck, *Acta Biomater.*, 2013, **9**, 6360–6368.
- 120 A. Casteren and J. Codd, *J. Insect Sci.*, 2010, **10**, 1–12.
- 121 W. Hansen and K. Autumn, *Proc. Natl. Acad. Sci. U. S. A.*, 2005, **102**, 385–389.
- 122 C. J. Clemente, J. M. R. Bullock, A. Beale and W. Federle, *J. Exp. Biol.*, 2010, **213**, 635–642.
- 123 N. Crawford, T. Endlein and W. J. P. Barnes, *J. Exp. Biol.*, 2012, **215**, 3965–3972.

